Cyclization of Hydrocarbon Chains Attached to a Planar Chromophore

Douglas S. Saunders[23] and Mitchell A. Winnik*

Lash Miller Laboratories and Departments of Chemistry, Erindale College and University of Toronto, Toronto, Canada M5S 1A1. *Received June 23, 1977*

ABSTRACT: A diamond-lattice model and Monte-Carlo methods are used to simulate cyclization of hydrocarbon chains up to 30 carbons in length attached to a bulky aromatic chromophore. The chromophore is modeled in the lattice by specifying as occupied those sites which best resemble its geometry. Cyclization is detected at a site adjacent to the chromophore (called the "reactive volume") somewhat remote from where the chain is attached. Furthermore, a chain which has any element in the reactive volume is deemed as cyclized. These choices simulate intramolecular photohydrogen abstraction reactions in *n*-alkyl esters of benzophenone 4-carboxylate. Partition functions are calculated separately for both cyclized and all chains. Their ratio, the cyclization probability P_n, is estimated at several temperatures for real hydrocarbon chains ($E_g = E_t + 500$ cal/mol) and for hypothetical chains biased to favor gauche rotamers ($E_g = E_t$ and $E_g = E_t - 500$ cal/mol). For the system under consideration, cyclization probability is relatively insensitive to extremes of temperature and to the statistical weights given gauche rotamers in the chain.

When a hydrocarbon chain is attached to a large bulky chromophore certain regions of space are no longer accessible to the chain. The substituent excludes a volume of space that would be available to an unsubstituted chain, and this steric effect must manifest itself in the conformational properties of the chain. One might imagine that various conformational properties of the chain might be differently sensitive to the presence of the chromophores. One might speculate that chain properties sensitive primarily to more extended chain configurations, like the mean-squared end-to-end distance[1] $\langle r^2 \rangle$ and higher even moments of **r**, might be relatively insensitive to the chromophore. On the other hand, chain properties more sensitive to compact configurations (cyclization, the persistence vector[2] **a**, and inverse moments[3] of **r**) might be much more sensitive both to the presence and the nature of the terminal substituent.

Cyclization probability[4] should be the conformational property of flexible chains most sensitive to interactions between remote chain elements and to substituents attached to the chain. There is chemical evidence from the early work of Carothers, Ziegler, and others on medium size ring formation (10 to 16 carbons) that transannular interactions between CH_2 groups affect cyclization of the chain termini.[5] On the other hand, the presence of oxygens or sp^2 carbons in the chain mitigate some of these remote interactions, and the odd–even alternating effect in those particular cyclization reactions disappears. We are interested in determining what factors affect the cyclization of hydrocarbon chains.

In this paper, we explore aspects of cyclization of hydrocarbon chains substituted at one end by a bulky planar chromophore. The approach taken is that of conformational calculations based upon a model which allows the bulk of the terminal substituent to be accomodated and which also excludes chain configurations in which one element of the chain would interfere sterically with a second element of the chain. Thus, within the context of the model, excluded volume considerations are taken into account.

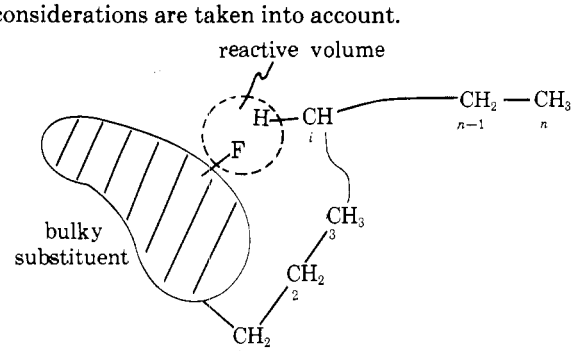

(I)

We conceptualize the problem in I. The bulky substituent is indicated, and C_1 serves as a convenient origin for our coordinate system. Since, experimentally, cyclization is detected by chemical reactions, we call the volume (labeled F) in which one would detect cyclization the "reactive volume". In a simple polymer not appended to a substituent, the reactive volume would be adjacent to C_1.

One can consider three kinds of cyclization probability for chains attached to a substituent. (i) One could focus on the probability that the chain terminus, the methyl group *n*, occupies the volume of space designated to imply cyclization (F in I); (ii) one could consider the probability $P_{i,n}$ that the *i*th CH_2 group in an *n*-carbon chain occupied that volume; or (iii) one could consider the sum of probabilities $P_n = \Sigma_i P_{i,n}$ that any chain element occupied the volume *F*.

In this paper, we describe the effects of chain length, temperature, and the gauche-trans rotational energy difference on those kinds of cyclization probability described by (ii) and (iii). Our choice is based upon the availability of experimental evidence closely related to $P_{i,n}$ and P_n.[6] These form a basis from which predictions of our model may be evaluated.

The model involves random walks on a tetrahedral lattice with second neighbor exclusions. Monte-Carlo techniques coupled with the sampling method of Rosenbluth and Rosenbluth[7] are used to compute averaged properties of the chains. The terminal substituent is accomodated by assigning as occupied those lattice sites which best describe its geometry. Certain lattice sites are chosen to simulate the reactive volume *F* in I. Chains passing through this volume are counted as cyclized chains. Properties of cyclized chains are compared with those of all chains. Values of $P_{i,n}$ and P_n are obtained from the appropriate estimated partition functions.

Similar models have been used by Smith[8] and by Bothorel[9] to calculate various properties of the *n*-alkanes. Smith used exact enumeration methods to evaluate selected properties of hydrocarbon chains up to 18 carbons and Monte-Carlo techniques to examine longer chains.[8] Several authors[10–14] have used off-lattice methods to explore properties of these chains. Sisido focused on cyclization probability for chains up to 16 carbons and demonstrated the importance of taking account of excluded volume in evaluating cyclization probabilities. With the exception of the very sophisticated model of Lal and Spencer,[11a] these calculations considered threefold rotational states about carbon–carbon bonds. The degree to which predictions of such models differ for such short chains from predictions based upon diamond lattice models is not known. The major difference between the models is the distortion of the CCC bond angle from 112 to 109.5° on the lattice.

0024-9297/78/2211-0025$01.00/0

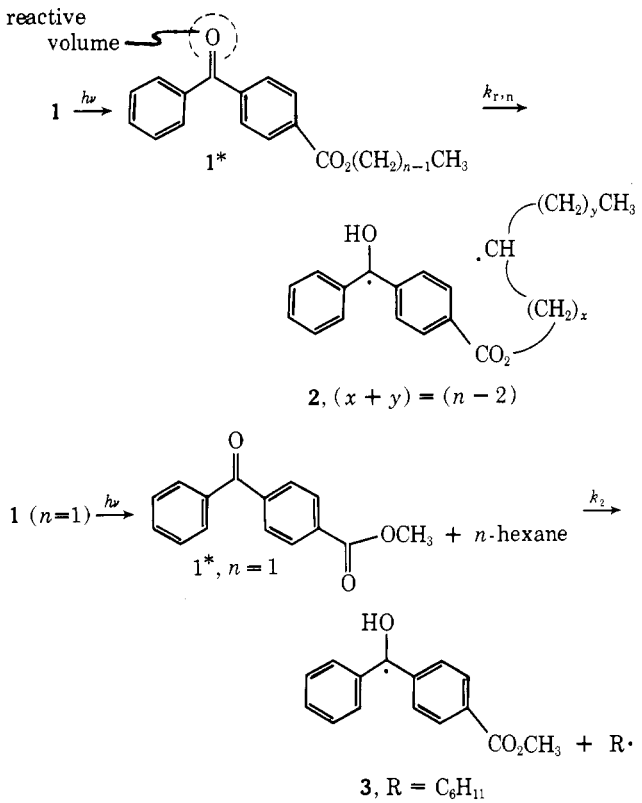

The molecules we consider are the n-alkyl esters of benzophenon 4-carboxylate, **1**. The intramolecular photochemistry of these molecules has been studied in some detail in our laboratory.[6b,15] Rate constants $k_{r,n}$ were obtained with high precision for the intramolecular hydrogen abstraction reaction $1 \rightarrow 2$, a process involving cyclization of the chain to occupy the reactive volume in 1*. P_n cannot be obtained directly from these results. Rather, we compared values of $k_{r,n}$ with that of k_2, the rate constant for the corresponding bimolecular hydrogen abstraction reaction. The ratio ($k_{r,n}/k_2 = C_{eff}$), the effective concentration,[16] has units of molarity. It is proportional to P_n and can be related to P_n if reasonable assumptions are made about the size of the reactive volume in 1*. When these assumptions are made, the similarity between experimental values of C_{eff} and those calculated from P_n is quite good.[15] Thus the model has had some success at simulating experimental phenomena.

Methodology and Semiempirical Considerations

(a) Structural Parameters. To describe the hydrocarbon chains, we examined self-avoiding walks on a diamond lattice with second-neighbor exclusions. Some structural parameters (the bond angle θ between successive CH_2 units and the rotational angle ϕ) are dictated by the lattice. Others were introduced empirically: the C–C bond length l and the energy difference $E_G = E_g - E_t$ for gauche and trans rotamers of the chain. Successive gauche bonds of the opposite sense are prohibited by the second-neighbor exclusion feature of the random walks. Following Flory,[2] we used a value of 500 cal/mol for E_G.

The ester group in the substituent is known to be planar. Steric and dipolar effects keep it in the trans configuration. Thus, only that configuration is considered in this work (see Figure 1). The asymmetry of the benzoyl group in the substituent gives rise to two rotamers about the ester group of virtually identical energy. These place the chain bearing oxygen either syn or anti to the ketone carbonyl in the substituent. We generate equal numbers of chains from the syn and anti ester groups and weight them equally in all calculations.

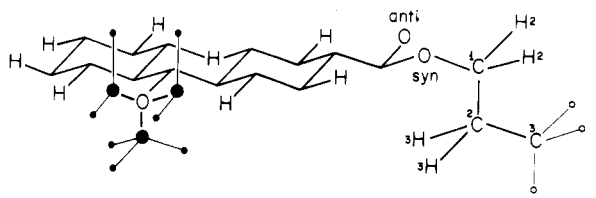

Figure 1. Diamond-lattice model of benzophenone 4-CO_2-$(CH_2)_{n-1}CH_3$ showing the first three carbons of the n-alkyl ester. The benzophenone rings and the ester group are coplanar. The two rotamers of the ester group are designated syn or anti with respect to the keto oxygen, and the ester is in the trans configuration. Equal numbers of chains are grown from each rotamer. The first three carbons in the chain are labeled C_1, C_2, C_3. The circles (○) indicate possible loci for C_4. The sites designated (●) represent the three inner hit sites; those designated (●) represent the seven outer hit sites. If any of these sites are occupied by an H from a CH_2 group, that chain is counted as in a reactive (hitting) conformation.

The addition of a bulky substituent to one end of the chain changes the rotational energy potentials of the first three methylene groups from those of an unsubstituted polymethylene chain. The ester group plays the major role in these changes.

Flory has examined the relative energies of the rotamers about the O–CH_2 bond in his work on poly(ethylene terephthalate).[18] Gauche rotamers place the second methylene group 2.83 Å from the carbonyl oxygen, within the sum of their respective van der Waals radii ($r_{CH_2} + r_O$) = 1.7 + 1.5 = 3.2 Å). Flory calculates that there are 400 cal of extra energy, relative to the trans orientation, associated with these rotamers. The uncertainty of the calculation, and the convenience of treating this interaction in a manner similar to gauche methylenes within unsubstituted polymethylene chains, has led us to assign E_G = 500 cal/mol to these gauche rotamers.

The interactions of a methylene group and an ether oxygen, separated by three bonds, have been examined by Mark in his studies of poly(ethylene oxide) and poly(tetramethylene oxide).[19,20] In a detailed analysis of these chains, he assigned a stabilization energy to the gauche rotamers of 200 cal/mol, relative to a methylene group oriented trans. He suggests that this is a result of small coulombic interactions between the methylene group and the oxygen, separated by 2.9 Å. Steric repulsions, he postulates, are unimportant at this distance. Comparison of his theoretical work with experiment suggests that gauche and trans rotamers could be isoenergetic (i.e., $E_g = -200 \pm 200$ cal). Since, experimentally, polyoxyalkanes are not as well understood as polymethylene chains, the present work assigns gauche and trans states of this step equal statistical weights.

Certain conformations about bonds (i), ($i + 1$), and ($i + 2$) place C(4)H_2 of the chain rather close to the ester oxygen to which C(1)H_2 of the chain is attached. In these conformations, the bonds ($i + 1$) and ($i + 2$) are $g^{\pm}g^{\mp}$. Mark has analyzed an identical geometry in poly(tetramethylene oxide).[19] He suggested that these conformations are destabilized by an additional 340 ± 250 cal/mol. Because of the large uncertainty in this value,[20] we choose for simplicity to assign 500 cal/mol to each gauche conformation in the sequence.

(b) The Chains and the Substituent. A diamond lattice is not an ideal framework for simulating the bulk of a planar chromophore; nevertheless, by designating as occupied those vertices which best correspond to the shape of the chromophore, one can map out a region of space similar in shape to that of the substituent under consideration. In this work, benzophenone 4-carboxylate could be simulated by dicyclohexyl ketone 4-carboxylate, in which only the equitorial hydrogens were kept in the lattice model, Figure 1. Space-filling models show a remarkable similarity in the shapes of the

Table I
Cyclization Probability $P_n^{(i)}$ vs. Chain Length[a] (Inner Hits)

Chain length	$E_t < E_g$,[b] T = −20 °C	$E_t < E_g$,[b] T = 25 °C	$E_t = E_g$[c]	$E_g < E_t$,[b] T = 25 °C	$E_g < E_t$,[b] T = −75 °C	$E_g < E_t$,[b] T = −128 °C
12	4.89 (±0.23)	4.50 (±0.20)	1.82 (+0.01)	0.39 (±0.01)	0.15 (±0.01)	0.04
14	10.17 (±0.41)	9.66 (±0.33)	6.17 (±0.10)	2.86 (±0.06)	1.75 (±0.06)	0.97 (±0.07)
16	12.87 (±0.55)	13.00 (±0.43)	10.66 (±0.13)	6.17 (±0.11)	4.15 (±0.12)	2.41 (±0.13)
18	15.99 (±0.85)	16.60 (±0.63)	15.76 (±0.17)	11.26 (±0.18)	9.86 (±0.28)	6.31 (±0.39)
20	20.02 (±1.13)	20.76 (±0.86)	20.73 (±0.21)	16.70 (±0.26)	14.25 (±0.45)	11.04 (±0.75)
22	23.11 (±1.42)	24.04 (±1.06)	25.20 (±0.25)	22.30 (±0.35)	21.34 (±0.86)	21.05 (±1.52)
24	26.14 (±1.81)	27.00 (±1.34)	28.98 (±0.28)	26.21 (±0.41)	24.49 (±0.93)	20.26 (±1.75)
26	33.45 (±3.87)	32.66 (±2.58)	32.35 (±0.30)	30.09 (±0.40)	26.73 (±0.95)	20.41 (±1.82)
28	38.73 (±6.03)	36.58 (±3.62)	35.29 (±0.33)	33.89 (±0.47)	30.09 (±1.00)	22.62 (±1.89)
30	37.37 (±7.05)	36.21 (±4.29)	35.98 (±0.35)	34.56 (±0.49)	30.43 (±1.07)	21.49 (±1.95)

[a] Values ×10⁴; parentheses contain error estimates, reported as 2σ. [b] Values reported are: Z (hitting chains)/Z (all chains); ΔE = 0.5 or −0.5 kcal/mol. [c] For $E_t = E_g$, values reported are also equal to (estimated number of hitting chains)/(estimated number of all chains).

Table II
Cyclization Probability $P_n^{(o)}$ vs. Chain Length[a] (Outer Hits)

Chain length	$E_t < E_g$,[b] T = −20 °C	$E_t < E_g$,[b] T = 25 °C	$E_t = E_g$[c]	$E_g < E_t$,[b] T = 25 °C	$E_g < E_t$,[b] T = −75 °C	$E_g < E_t$,[b] T = −128 °C
11	1.41 (±0.05)	1.44 (±0.05)	1.34 (±0.03)	1.03 (±0.02)	0.90 (±0.02)	0.79 (±0.03)
13	2.93 (±0.10)	3.05 (±0.08)	2.93 (±0.04)	2.09 (±0.03)	1.65 (±0.03)	1.25 (±0.05)
15	4.17 (±0.15)	4.41 (±0.12)	4.59 (±0.05)	3.61 (±0.04)	3.00 (±0.05)	2.35 (±0.08)
17	5.08 (±0.18)	5.50 (±0.16)	6.27 (±0.06)	5.34 (±0.06)	4.66 (±0.06)	3.96 (±0.18)
19	6.01 (±0.25)	6.47 (±0.20)	7.67 (±0.06)	7.03 (±0.07)	6.53 (±0.16)	6.12 (±0.36)
21	6.60 (±0.30)	7.17 (±0.24)	8.92 (±0.08)	8.57 (±0.10)	8.20 (±0.22)	7.62 (±0.48)
23	7.56 (±0.55)	8.07 (±0.36)	9.95 (±0.08)	9.84 (±0.10)	9.38 (±0.25)	8.36 (±0.50)
25	8.41 (±0.55)	8.93 (±0.40)	10.86 (±0.08)	10.95 (±0.11)	10.22 (±0.24)	8.24 (±0.52)
27	9.09 (±0.70)	9.53 (±0.52)	11.66 (±0.09)	11.88 (±0.13)	11.30 (±0.30)	9.76 (±0.64)
29	9.32 (±0.98)	9.96 (±0.78)	12.37 (±0.10)	12.79 (±0.14)	12.31 (±0.35)	10.52 (±0.80)

[a] Values ×10³; parentheses contain error estimates, reported as 2σ. [b] Values reported are: Z (hitting chains)/Z (all chains); ΔE = 0.5 or −0.5 kcal/mol. [c] For $E_t = E_g$, values reported are also equal to (estimated number of hitting chains)/(estimated number of all chains).

chromophore and its model.[21]

Chains were grown stepwise from the ester oxygen as indicated in Figure 1. C_1 was placed in the trans geometry with respect to the ester. C_2 was placed at random in one of the three lattice sites adjacent to C_1. The remaining valences on C_1 were then designated as occupied by hydrogens. C_3 was then added at random to one of the lattice sites adjacent to C_2; then its valences were completed with the addition of hydrogens. In this manner, chains were grown up to 30 carbons.[21] To sample all chains attached to the substituent, two samples of 180 000 chains were grown. One sample was grown from the syn conformation of the ester and the other was grown from the anti conformation. In addition, separate samples of nearly 400 000 chains were grown with a pseudopotentional importance sampling technique[21] to generate 60 000 cyclized chains from each conformer of the ester.

Chains were grown with the probability of choosing a gauche step, p_g, equal to p_t, that of choosing a trans step. Under these conditions, $E_g = E_t$. The coordinates of each carbon and its step weight were stored on magnetic tape. Real temperatures were introduced into the calculations by reweighting gauche vectors by a factor of $\exp(-500/RT)$. Monte-Carlo methods were used to estimate properties of the chains. Details of the calculation of the standard deviation in P_n are described in the Appendix.

(c) Detecting Cyclization. Figure 1 shows the lattice representation of the substituent from which samples of chains were grown. Cyclization was detected by identifying those chains which had an H from a CH_2 group occupy one of the lattice sites designated as reactive. We call those sites "hit sites" and the chains which pass through them "hitting chains". Ten such sites are indicated in Figure 1. These surround the ketone carbonyl oxygen. Because only even-membered rings may be formed on a tetrahedral lattice, we could count separately those chains that occupy one of the three hit sites adjacent to the reactive oxygen from those that occupy the outer tier of seven hit sites. By comparing the partition functions of chains passing through the inner hit sites with those passing through the latter, outer, hit sites, we get some indication of the sensitivity of cyclization to the size of the volume designated as reactive.

Results and Discussion

In the photochemical reactions of **1**, hydrogen abstraction can be detected only at the CH_2 groups in the chain; the methyl groups are negligibly reactive. Therefore, we define the cumulative cyclization probability P_n as the sum of cyclization probabilities $P_{i,n}$ for each of the $(n-1)$ CH_2 groups in the chain. We can consider two classes of cyclized chains. For those that have an H from a CH_2 group occupying one of the three lattice sites adjacent to the reactive oxygen hit at the "inner hit sites", we denote the cyclization probability of these chains as $P_n^{(i)}$. For those that have a methylene hydrogen occupying one of the adjacent tier of seven lattice sites, the "outer hit sites", we denote the cyclization probability as $P_n^{(o)}$. When we wish to consider the partition function for the separate classes of chains which occupy the inner or outer hit sites, we shall use the superscript forms $Z_o^{(i)}$ and $Z_o^{(o)}$, respectively.

The cyclization probability is equal to the ratio of partition functions for cyclized chains and all chains. In the special case that $E_g = E_t$, the partition functions become simply the

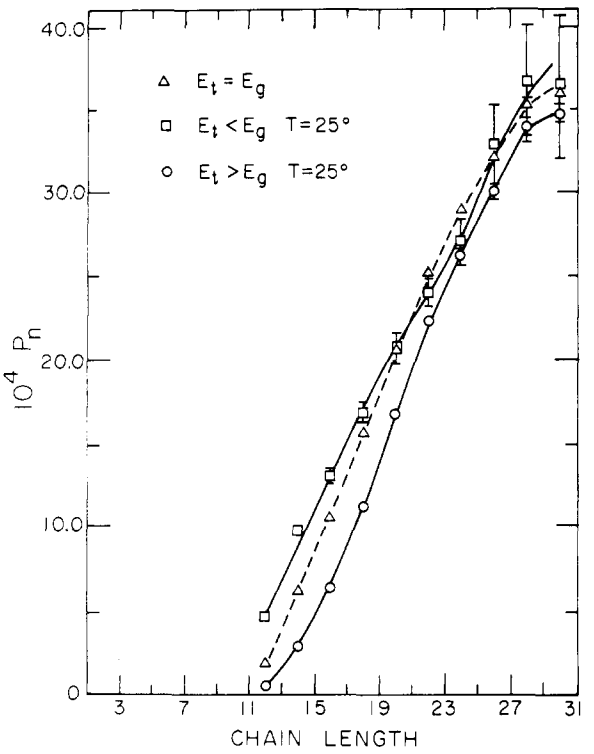

Figure 2. The chain length dependence of the cyclization probability $P_n^{(i)}$ at the inner hit sites for n-alkyl esters of benzophenone 4-carboxylate: (△) $E_t = E_g$; (□) $E_g = E_t + 500$ cal/mol, 25 °C; (○) $E_g = E_t - 500$ cal/mol, 25 °C. The error bars represent two standard deviations.

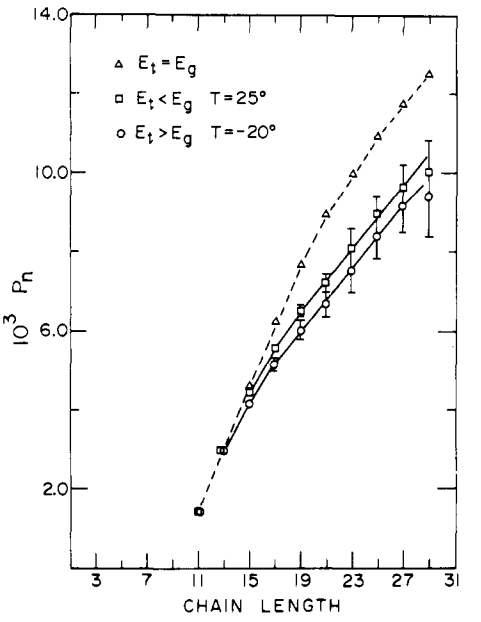

Figure 3. The chain length dependence of cyclization probability $P_n^{(o)}$ at the outer hit sites for (△) $E_t = E_g$; (□) $E_g = E_t + 500$ cal/mol, 25 °C, and (○) −20 °C.

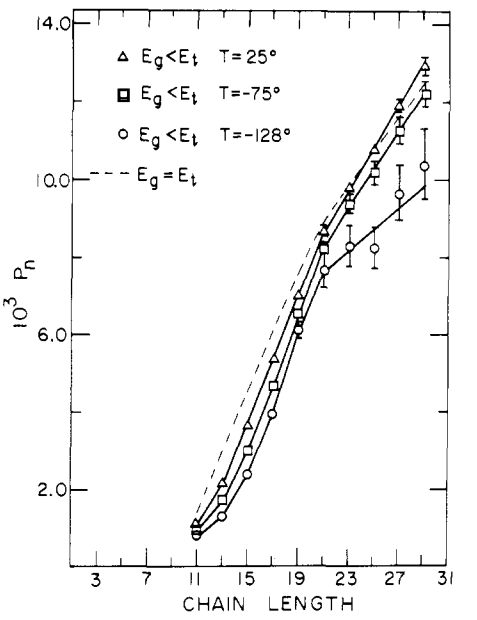

Figure 4. The chain length dependence of cyclization probability $P_n^{(o)}$ at the outer hit sites under the hypothetical conditions that $E_g = E_t - 500$ cal/mol: (△) 25 °C, (□) −75 °C, (○) −128 °C.

number of conformations accessible to any class of chains.

In our calculations, the energy differences between gauche and trans rotamers ($E_G = E_t - E_g$) were taken to be 0, ±500 cal/mol. When $E_G = 0$, one examines the consequences of second-neighbor avoiding walks on the tetrahedral lattice. When $E_G = +500$ cal/mol, one simulates real hydrocarbon chains. At the other extreme, when $E_G = -500$ cal/mol, one explores a hypothetical situation. By favoring gauche rotamers in this way, one gains some insight into the property of hydrocarbon chains distorted from their natural conformation. One also explores the sensitivity of chain properties to drastic differences in simulated conditions.

(a) Cumulative Cyclization Probability. Tables I and II compile estimated P_n values for several temperatures as a function of chain length. Included are results from chain samples reweighted to favor trans ($E_t < E_g$) and gauche rotamers ($E_g < E_t$) and from unreweighted chain samples, where neither rotamer is favored ($E_t = E_g$).

The $P_n^{(i)}$ values in Table I are based on hits at the three inner hit sites; $P_n^{(o)}$ values in Table II represent hits at the seven outer hit sites. The brackets beneath each estimate contain the associated standard deviation values. Estimates of P_n from the reweighted samples have much larger standard deviation values than those of the unreweighted samples. Increases in the deviation values correspond to the degree of reweighting in the sample.

Values of $P_n^{(o)}$ are significantly larger, per site, than values of $P_n^{(i)}$. While we did not count hitting chains separately at each site, values of $P_n^{(o)}$ are larger than $\frac{7}{3}P_n^{(i)}$ by as much as 40%. This result implies that there is a nonuniform probability of finding CH_2 groups occupying inner and outer hit sites. An effect, probably steric in origin, limits the number of ways a chain can approach close to the reactive carbonyl oxygen. There are a greater number of ways in which it can approach the outer hit sites.

As we shall emphasize below, the major feature of the data in Tables I and II is the relative insensitivity of the cyclization probability to drastic changes in temperature or assumed values of E_G. For example, for realistic chains cyclizing at the inner hit sites, a change of temperature from infinity, where $E_g = E_t$, to −20 °C causes noticeable changes in P_n only for rather short chains. Somewhat larger changes occur for hits at the outer hit sites, but these, too, are small. The largest changes in P_n are still less than 40%. They occur for the hypothetical chains whose gauche rotamers are favored by 0.5 kcal/mol and only then at very low temperatures.

In Figure 2, the cumulative cyclization probability $P_n^{(i)}$ is plotted against chain length for three conditions: $E_g = E_t + 500$ cal/mol at 25 °C, $E_g = E_t$ and $E_g = E_t - 500$ cal/mol at 25 °C. These are chains for which cyclization is detected at the inner hit sites. The insensitivity of P_n to such extremes of

Table III
Internal Distribution of Hits within Hitting Chains (Inner Hits)

16-Carbon chains				20-Carbon chains					
	Hit site				Hit site				
Weighting	11	13	15	Weighting	11	13	15	17	19
$E_t < E_g$[a]	22.4[b]	34.2	43.5	$E_t < E_g$	15.3	20.1	17.4	20.2	27.3
$T = 25$ °C	(±1.7)	(±2.2)	(±2.4)	$T = 25$ °C	(±1.9)	(±2.0)	(±1.3)	(±1.6)	(±2.4)
$E_t = E_g$	12.0	32.1	55.9	$E_t = E_g$	6.2	16.0	19.1	22.9	35.8
	(±0.45)	(±0.80	(±1.2)		(±0.25)	(±0.40)	(±0.45)	(±0.50)	(±0.80)
$E_g < E_t$[a]	4.7	29.8	65.5	$E_g < E_t$	1.6	10.9	17.2	24.8	45.6
T = 25 °C	(±0.18)	(±1.0)	(±1.8)	$T = 25$ °C	(±0.08)	(±0.40)	(±0.60)	(±0.80)	(±1.3)

28-Carbon chains									
	Hit Site								
Weighting	11	13	15	17	19	21	23	25	27
$E_t < E_g$	8.3	14.4	8.8	12.1	10.6	10.1	8.1	11.9	15.4
$T = 25$ °C	(±2.6)	(±3.8)	(±1.2)	(±1.6)	(±1.7)	(±2.3)	(±1.5)	(±5.5)	(±5.9)
$E_t = E_g$	3.6	9.2	10.7	13.4	13.6	12.6	11.5	10.2	15.1
	(±0.17)	(±0.30)	(±0.30)	(±0.35)	(±0.34)	(±0.38)	(±0.35)	(±0.30)	(±0.40)
$E_g < E_t$	0.8	5.2	8.2	11.5	14.0	15.0	13.1	12.8	19.4
$T = 25$ °C	(±0.05)	(±0.20)	(±0.30)	(±0.40)	(±0.50)	(±0.60)	(±0.50)	(±0.45)	(±0.80)

[a] $\Delta E = +0.5$ or -0.5 kcal/mol. [b] Percent hits at each site; parentheses contain error estimates, reported as 2σ.

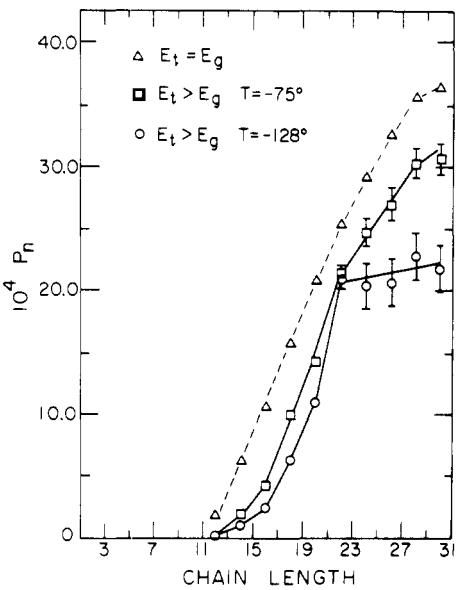

Figure 5. The chain length dependence of the cyclization probability $P_n^{(i)}$ at the inner hit sites for the hypothetical conditions $E_g = E_t - 500$ cal/mol: (□) −75 °C, (○) −128 °C, (△) $E_t = E_g$.

conditions was very surprising to us. Since $P_n^{(i)} = Z_o^{(i)}/Z_t$, these results require that the partition functions $Z_o^{(i)}$ and Z_t have very similar dependence on E_G and temperature.

Values of $P_n^{(o)}$ for chains passing through the outer hit sites are plotted vs. chain length in Figures 3 and 4. The former graph describes cyclization of realistic chains ($E_g = E_t + 500$ cal/mol) at 25 and −20 °C and compares them to chains in which gauche and trans rotamers are equally weighted ($E_g = E_t$). Cyclization probability is modestly sensitive to changes in temperature. A decrease in temperature from ∞($E_g = E_t$) to 25 °C causes a 18 to 20% decrease in $P_n^{(o)}$.

When the chains are reweighted to favor strongly the gauche rotamers, the cumulative cyclization probability decreases and the shapes of the P_n vs. chain length plots change markedly. The changes are more modest at the outer hit sites, Figure 4, than at the inner hit sites, Figure 5. In both cases, the curves become sigmoidal functions of chain length. The sudden increase in P_n with n, observed at carbons 11 and 12 when $E_g \geq E_t$, is shifted to longer n when $E_g < E_t$. The effect is even more pronounced at lower temperatures where the gauche rotamers have large statistical weights. Under these conditions, chains with large fractions of gauche bonds count heavily in the estimation of the partition functions Z_o and Z_T.

It is the Z_o term which is more affected by the reweighting. Chains which have large fractions of gauche bonds find relatively few pathways to reach the volume of space at which cyclization is detected. For chains longer than 21 carbons, cyclization is possible, but it does not increase as rapidly with chain length as it would for chains with larger fractions of trans bonds.

It appears that chains with large fractions of gauche bonds are directed into the space away from the chromophore. They must follow rather circuitous pathways in order to reach the reactive volume and not interfere sterically with the chromophore itself.

(b) Internal Distribution of Hits within Chains. Within each chain of n carbons, each of the $(n - 1)$ CH_2 groups is capable of reacting chemically with the photoexcited ketone carbonyl oxygen in **1**. Correspondingly, $P_{i,n}$ describes the probability that the ith CH_2 group in an n carbon chain has an H in the reactive volume in **1**. Analyses of these $P_{i,n}$ values provide further insights into cyclization processes of the chain.

We focus on the inner hit sites and consider the three extremes of conditions: $E_g = E_t + 500$, $E_g = E_t$, and $E_g = E_t - 500$ cal/mol. The internal distributions of hits for three representative chain lengths, 16-, 20-, and 28-carbon chains, are shown in Table III. As in the case of P_n estimates, there are substantial increases in standard deviations for reweighted samples.

The relative probabilities of cyclization for each CH_2 group are presented graphically for 16-carbon chains in Figure 6 and for 20- and 28-carbon chains in Figure 7. The distribution of hitting carbons is narrow for 16-carbon chains and very broad for 28-carbon chains. For real chains ($E_g > E_t$), two maxima appear in the plots of $P_{i,n}$ vs. carbon number for chains of 20 or more carbons. One occurs in the middle of the chain, near C-13, its exact position depending upon temperature. The other maximum occurs near the chain end. This maximum,

Table IV: Average Number of Gauche Bonds in the Sample of Hitting Chains (Excluding the Conformation of the C(2)–C(3) Bond)

Chain length	Chain origin	Hit type	Hit site on the chain																	
			10	11	12	13	14	15	16	17	18	19	20	21	22	23	24	25	26	27
16 carbons (7.18 ± 0.05)[b]	Syn	Inner		5.76[a]		6.72		7.04												
		Outer	7.05		7.00		7.20													
	Anti	Inner				6.19		6.77												
		Outer	6.72		6.68		7.03													
20 carbons (9.17 ± 0.07)	Syn	Inner		7.67		8.75		9.07		9.15		9.39								
		Outer	9.04		8.93		9.19		9.26		9.39									
	Anti	Inner				8.28		9.26		9.52		9.71								
		Outer	8.88		8.71		9.03		9.18		9.36									
24 carbons (11.15 ± 0.10)	Syn	Inner		9.65		10.75		11.07		11.12		11.34		11.41		11.50				
		Outer	11.04		10.93		11.13		11.20		11.33		11.44		11.60					
	Anti	Inner				10.28		10.81		10.99		11.21		11.35		11.52				
		Outer	10.87		10.75		11.10		11.12		11.37		11.49		11.50					
28 carbons (13.14 ± 0.13)	Syn	Inner		11.66		12.74		13.06		13.05		13.38		13.39		13.45		13.48		13.48
		Outer	13.0		12.96		13.19		13.20		13.26		13.38		13.55		13.51		13.44	
	Anti	Inner				12.06		12.77		12.97		13.19		13.36		13.43		13.35		13.50
		Outer	12.85		12.70		13.09		13.07		13.30		13.42		13.50		13.42		13.62	

[a] Average number of gauche bonds in the sample of 16-carbon chains which hit at C(11). [b] Average number of gauche bonds in the sample of all 16-carbon chains.

Table V: Average Number of Gauche Bonds in the Sample of Hitting Chains (Including the Conformation about the C(2)–C(3) Bond)

Chain length	Chain origin	Hit type	Hit site on the chain																	
			10	11	12	13	14	15	16	17	18	19	20	21	22	23	24	25	26	27
16 carbons (7.77 ± 0.05)[b]	Syn	Inner		6.76[a]		7.72		7.99												
		Outer	8.05		7.97		8.00													
	Anti	Inner				7.19		7.69												
		Outer	7.72		7.61		7.71													
20 carbons (9.77 ± 0.07)	Syn	Inner		8.67		9.75		10.02		9.91		10.05								
		Outer	10.04		9.91		10.04		9.90		9.98									
	Anti	Inner				9.28		9.69		9.70		9.79								
		Outer	9.88		9.63		9.74		9.70		9.82									
24 carbons (11.75 ± 0.09)	Syn	Inner		10.65		11.75		12.01		11.86		11.97		11.96		12.02				
		Outer	12.05		11.91		11.95		11.84		11.92		11.98		12.08					
	Anti	Inner				11.28		11.73		11.66		11.73		11.81		11.95				
		Outer	11.87		11.67		11.82		11.64		11.82		11.94		11.92					
28 carbons (13.73 ± 0.11)	Syn	Inner		11.66		12.74		13.06		13.05		13.38		13.39		13.45		13.48		13.48
		Outer	14.00		13.94		14.01		13.83		13.85		13.91		14.00		13.98		13.93	
	Anti	Inner				13.06		13.69		13.63		13.70		13.82		13.85		13.74		13.93
		Outer	13.85		13.62		13.81		13.60		13.76		13.87		13.91		13.83		13.99	

[a] Average number of gauche bonds in the sample of 16-carbon chains which hit at C(11). [b] Average number of gauche bonds in the sample of all 16-carbon chains.

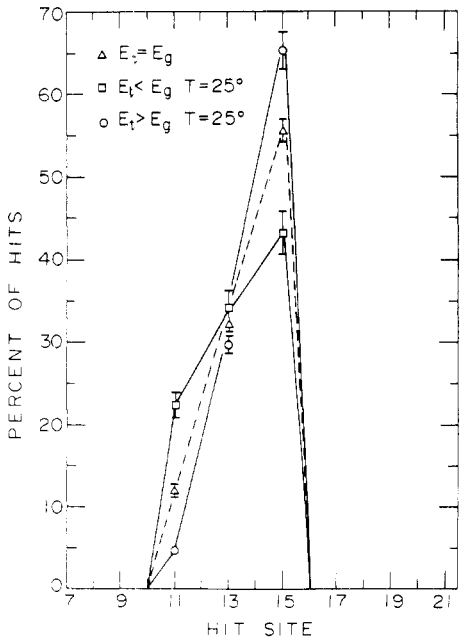

Figure 6. Relative distribution of hits among the carbons of a 16-carbon chain attached to the benzophenone 4-carboxylate substituent. Cyclization is detected at the inner hit sites in the model. Hits at the chain end, C_{16}, are not counted: (△) $E_t = E_g$; (□) $E_g = E_t + 500$ cal/mol, 25 °C; (○) $E_g = E_t - 500$ cal/mol, 25 °C.

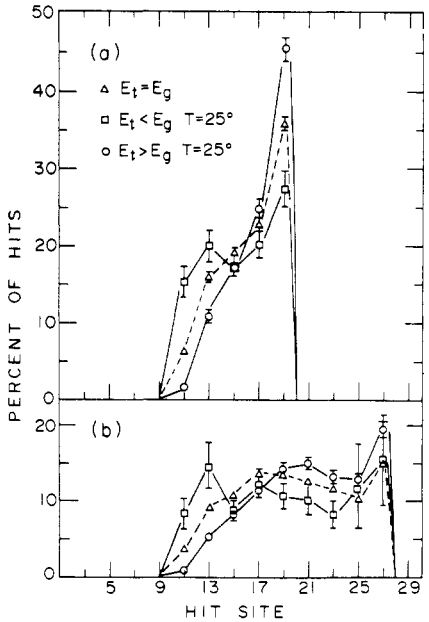

Figure 7. Relative distribution of hits among the carbons of (a) 20-carbon and (b) 28-carbon esters of benzophenone 4-carboxylate. Cyclization is detected at the inner hit sites, and hits at the chain ends are not counted. Symbols are as indicated for Figure 6.

which represents some kind of end-of-chain effect, appears in plots of $P_{i,n}$ vs. n for all chain lengths regardless of whether E_g is greater than or less than E_t. Its magnitude does depend upon temperature and the value of E_G.

Real chains at 25 °C, weighted to favor trans bonds, show a larger percentage of hits at low carbon number than chains weighted to favor gauche rotamers. The latter show pronounced increases in the fraction of hits which occur at higher carbon number. Thus chains which undergo cyclization at low carbon number appear to have a larger fraction of trans bonds than chains which cyclize at high carbon number. Chains with large fractions of gauche rotamers have few hits at carbons 11 and 13 but show increasing amounts of cyclization further along the chain.

(c) Fraction of Gauche Bonds. In order to pinpoint the peculiar behavior of the hydrocarbon chains in the model toward cyclization, we have examined the number of gauche bonds in all chains and in various subclasses of cyclized chains. In counting gauche bonds, we neglected the rotational state of the bond between C_2 and C_3, since this bond was not reweighted by $\exp(\pm 500/RT)$ in the above calculations. For convenience, we define $\langle G_n \rangle_o^{(i)}$ and $\langle G_n \rangle_o^{(o)}$ to be the average number of gauche bonds in hitting chains of length n, occupying inner and outer hit sites, respectively. Similarly, $\langle G_n \rangle_t$ is the weighted average of gauche bonds in the sample of all chains of length n.

Table IV gives $\langle G_n \rangle_o^{(i)}$ and $\langle G_n \rangle_o^{(o)}$ values for $n = 16$, 20, 24, and 28 carbons, as a function of hit site and chain origin (i.e., syn or anti oxygen (see Figure 1)). The brackets beneath the chain length values contain for comparison the corresponding $\langle G_n \rangle_t$ value for the sample of all chains of that length.

In general, $\langle G_n \rangle_o^{(i)}$ values increase as the reaction site occurs closer to the chain end. This is particularly true for chains of 16 and 20 carbons. Longer chains (24 and 28 carbons) also show this increase in $\langle G_n \rangle_o^{(i)}$ values for sites up to C(20). Beyond C(20), however, the value of $\langle G_n \rangle_o^{(i)}$ becomes approximately independent of hit site. This constant value for $\langle G_n \rangle_o^{(i)}$ is larger by about 0.3 gauche bonds than the corresponding $\langle G_n \rangle_t$ value for the sample of all chains.

The $\langle G_n \rangle_o^{(i)}$ values for chains hitting at C(11), C(13), and C(15), on the other hand, are 1.5 to 0.1 gauche bonds lower than the $\langle G_n \rangle_t$ value. On the average, chains which hit at the first possible site [C(11) for chains grown from the syn oxygen, and C(13) for those grown from the anti oxygen] have approximately 1.5 fewer gauche bonds than are found in the sample of all chains. Thus the shortest path to the carbonyl oxygen from the ester group requires about two extra trans bonds than are found, on the average, for chains sampling all space. This difference rapidly disappears with increasing hit site number.

In order to assess the importance of the rotational state of the C(2)–C(3) bond on cyclization, a separate estimate was made, including in the tabulation *all* gauche bonds in the chain. The results are shown in Table V for hitting chains, and in the brackets of Table V data for all chains.

Irrespective of chain length, the $\langle G_n \rangle_o^{(i)}$ values for chains registering hits at C(11), C(13), and C(15) increase by almost exactly one bond when the rotational state of the C(2)–C(3) bond is included. This is also true for $\langle G_n \rangle_o^{(o)}$ values for chains registering outer hits at C(10) and C(12). Chains hitting at sites near the first hit site *require* the third step to be gauche.

There is no such restriction, however, for inner hitting chains registering hits beyond C(17), or for outer hitting chains with hit sites beyond C(14). These chains show increases in $\langle G_n \rangle_o^{(i)}$ and $\langle G_n \rangle_o^{(o)}$ values which are very similar to the increases in $\langle G_n \rangle_t$ values for the sample of all chains (approximately 0.6 gauche bonds).

The effect of reweighting on the cumulative cyclization probability P_n is the sum of reweighting effects on $P_{i,n}$. Inner hitting chains of fewer than 20 carbons have $\langle G_n \rangle_o^{(i)}$ values which are smaller than the corresponding $\langle G_n \rangle_t$ value for the sample of all chains of the same length. Reweighting in favor of trans bonds, therefore, increases $P_n^{(i)}$ for these chains. This effect is soon overcome for longer chains, since $\langle G_n \rangle_o^{(i)}$ values associated with hit sites near the chain end are larger than $\langle G_n \rangle_t$. The overall effect of reweighting on P_n for inner hitting chains is small (Figures 2 and 5).

Reweighting effects on P_n for outer hitting chains are modestly different (Figures 3 and 4). Short chains have hit sites with $\langle G_n \rangle_o^{(o)}$ values slightly below the corresponding $\langle G_n \rangle_t$ value. $P_n^{(o)}$ values are virtually unaffected by reweighting. Longer chains contain increasingly more hit sites with $\langle G_n \rangle_o^{(o)}$ values slightly larger than the $\langle G_n \rangle_t$ value. Thus reweighting in favor of trans bonds depresses the P_n values from those of the unreweighted sample for these chains. Reweighting in favor of gauche bonds compensates for the effect of early hit sites and P_n values remain unchanged except for extreme reweighting.

Conclusions

Vast changes in temperature or in the value of E_G have relatively small affects on cyclization of the hydrocarbon chain in the model. This insensitivity to changes in $\exp(-E_G/RT)$ derives from the similar fraction of gauche bonds in both cyclized chains and all chains attached to the chromophore. Thus while the partition functions for cyclized chains and all chains are sensitive to the value of $\exp(-E_G/RT)$, their ratio is not. Changes in cyclization probability become apparent only for extreme reweighting of the calculations to favor gauche or trans bonds.

Two factors affect cyclization of the chains into the reactive volume. The first is the bulk of the chromophore. Chains shorter than 11 carbons (outer hit sites) and 12 carbons (inner hit sites) are too short for cyclization to be detected. The large increase in cyclization probability with chain length for chains of 11 to 25 carbons is due to the increased number of pathways by which the chain can reach the reactive volume without encountering the chromophore.

The second factor is more subtle. For chains with large fractions of gauche bonds, cyclization is difficult. To cyclize at low carbon number, chains must have a substantial fraction of trans bonds, more than half. Consequently, short chains with large fractions of gauche bonds cannot reach the reactive volume. For chains longer than 20 carbons, this restriction disappears. Cyclization is still difficult, however. Even for 30 carbon chains hitting near the chain end, cyclization is favored for chains with equal numbers of gauche and trans rotamers.

One interesting result of the calculation is the discovery that chains which hit at low carbon number require the bond between carbons 2 and 3 to be in the gauche conformation.

Acknowledgment. The authors wish to thank the National Research Council of Canada and the Research Corporation for their generous financial support.

Appendix

The coefficient of variation in P_n ($CV(P_n)$) is obtained from the coefficients of variation for Z_o and Z_T according to eq 1, where $CV(\langle \hat{Z}_o \rangle) = [\sigma(\langle \hat{Z}_o \rangle)/\langle \hat{Z}_o \rangle] \times 100\%$, and $CV(\langle \hat{Z}_T \rangle)$ is similarly defined. The term $(\langle \hat{Z}_o \rangle)$ is the standard deviation in the estimated partition function Z_o and (Z_T) is that for Z_T. The standard deviation for the partition functions[22] of the total ensemble of chains is given by (2), where N is the sample size, W_i is the weight given to the i'th chain in the sample, and $\overline{W}$ is obtained from (3).

$$CV(P_n) = [CV^2(\langle Z_o \rangle) + CV^2(\langle Z_T \rangle)]^{1/2} \quad (1)$$

$$\sigma(\langle \hat{Z}_T \rangle) = \left[\frac{1}{N}\sum_{i=1}^{N}(W_i - \overline{W})^2\right]^{1/2} \quad (2)$$

$$\overline{W} = \frac{1}{N}\sum_{i=1}^{N} W_i \quad (3)$$

Calculation of the coefficient of variation for estimates of the partition functions of hitting chains is more complicated. Consider generating *only* a sample of M_o cyclized chains. Each chain in this sample has a probability p_j' and a corresponding weight W_j' such that

$$P_j' = \prod_{k=1}^{n} p_{kj}' \quad (4)$$

$$W_j' = (P_j')^{-1} \quad (5)$$

where p_j' is the probability of choosing the k'th step of the j'th chain.

Now consider this sample as part of the larger sample M of all chains. The cyclized chains now have a second set of probabilities P_l and weights W_l associated with them. The l subscript denotes the different numbering of these chains within the larger sample. The P_l for each cyclized chain is related to the P_j' for the chain by a factor which reflects the frequency of choosing a cyclized chain from among the sample of all chains: $P_l = (M_o/M)P_j'$ and $W_l = (M/M_o)W_j'$.

The partition function for cyclized chains can be estimated by eq 6, and the variance associated with the estimate, eq 7, may be expanded to yield (8).

$$\langle \hat{Z}_o \rangle = \overline{W}_o = \frac{1}{M_o}\sum_{j=1}^{M_o} W_j' \quad (6)$$

$$\mathrm{var}(\langle \hat{Z}_o \rangle) = \frac{1}{M_o}\sum_{j=1}^{M_o}(W_j' - \overline{W}_o)^2 \quad (7)$$

$$\mathrm{var}(\langle \hat{Z}_o \rangle) = \frac{1}{M_o}\sum_{j=1}^{M_o}(W_j')^2 - \left(\frac{1}{M_o}\sum_{j=1}^{M_o} W_j'\right)^2 \quad (8)$$

The variance can also be expressed in terms of the weights of the cyclized chains within the larger sample, where $\delta_l = 1$ if the chain appears in the sample of cyclized chains and is zero otherwise.

$$\mathrm{var}(\langle \hat{Z}_o \rangle) = \frac{1}{M_o}\sum_{l=1}^{M}\left(\frac{M_o}{M} W_l \delta_l\right)^2 - \left(\frac{M}{M_o}\sum_{l=1}^{M}\frac{M_o}{M} W_l \delta_l\right)^2$$

$$= \frac{M_o}{M^2}\sum_{l=1}^{M} W_l^2 \delta_l - \left(\frac{1}{M}\sum_{l=1}^{M} W_l \delta_l\right)^2 \quad (9)$$

References and Notes

(1) (a) H. Morawetz, "Macromolecules in Solution", 2nd ed, Wiley, New York, N.Y., 1975, Chapter III; (b) A. J. Hopfinger, "Conformational Properties of Macromolecules", Academic Press, New York, N.Y., 1973, Chapter 1.
(2) P. J. Flory, "Statistical Mechanics of Chain Molecules", Wiley, New York, N.Y., 1969, pp 111 and 401–3.
(3) J. J. Freire and A. Horta, *J. Chem. Phys.*, **65**, 4049 (1976).
(4) (a) J. A. Semlyen, *Adv. Polym. Sci.*, **21**, 42 (1976); (b) P. J. Flory, U. W. Sutter, and M. Mutter, *J. Am. Chem. Soc.*, **98**, 5733 (1976); (c) U. W. Sutter, M. Mutter, and P. J. Flory, *ibid.*, **98**, 5740 (1976); (d) M. Mutter, U. W. Sutter, and P. J. Flory, *ibid.*, **98**, 5745 (1976).
(5) For a review, see G. M. Bennet, *Trans. Faraday Soc.*, **37**, 794 (1941).
(6) (a) R. Breslow and M. A. Winnik, *J. Am. Chem. Soc.*, **91**, 3083 (1969); (b) M. A. Winnik, S. Basu, C. K. Lee, and D. S. Saunders, *ibid.*, **98**, 2928 (1976); (c) E. R. Eck, D. J. Hunter, and T. Money, *J. Chem. Soc., Chem. Commun.*, 865 (1974); (d) M. A. Winnik and D. S. Saunders, *ibid.*, 156 (1976).
(7) M. N. Rosenbluth and A. W. Rosenbluth, *J. Chem. Phys.*, **23**, 356 (1955).
(8) R. P. Smith, *J. Chem. Phys.*, **40**, 2963 (1964); **42**, 1162 (1965); **47**, 5364 (1967).
(9) C. Clement and P. Bothorel, *J. Chem. Phys.*, **61**, 1262 (1964).
(10) M. Sisido, *Macromolecules*, **4**, 737 (1971).
(11) (a) M. Lal and D. Spencer, *Mol. Phys.*, **22**, 649 (1971); (b) K. Suzuki and Y. Nakata, *Bull. Chem. Soc. Jpn.*, **43**, 1006 (1970).
(12) (a) R. L. Jernigan and P. J. Flory, *J. Chem. Phys.*, **50**, 4178, 4185 (1967).
(13) K. Nagai, *J. Chem. Phys.*, **47**, 4690 (1969).
(14) (a) P. Bothorel, J. Belle, and B. Lemaire, *Chem. Phys. Lipids*, **12**, 96 (1974); (b) P. Bothorel and J. Belle, *C. R. Hebd. Seances Acad. Sci., Ser C*, 437 (1976).
(15) (a) M. A. Winnik, *Acc. Chem. Res.*, **10**, 178 (1977); (b) M. A. Winnik, A. Lemire, D. S. Saunders, and C. K. Lee, *J. Am. Chem. Soc.*, **98**, 2000 (1976); (c) M. A. Winnik and A. Lemire, *Chem. Phys. Lett.*, **46**, 283 (1977).

(16) H. Morawetz, *Pure Appl. Chem.*, **38**, 267 (1974).
(17) (a) Reference 2, Chapter 3; (b) T. Shimonouchi, private communication.
(18) A. D. Williams and P. J. Flory, *J. Polym. Sci., Part A-2*, **5**, 399 (1967).
(19) (a) K. Bak, G. Elefante, and J. E. Mark, *J. Phys. Chem.*, **71**, 4007 (1967); (b) J. E. Mark, *J. Am. Chem. Soc.*, **88**, 3708 (1966); J. E. Mark, *J. Polym. Sci., Part B*, **4**, 825 (1966).
(20) Reference 2, p 173.
(21) (a) M. A. Winnik, R. E. Trueman, G. Jackowski, D. S. Saunders, and S. G. Whittington, *J. Am. Chem. Soc.*, **96**, 4843 (1974); (b) M. A. Winnik, D. Saunders, G. Jackowski, and R. E. Trueman, *ibid.*, **96**, 7510 (1974).
(22) F. L. McCrackin *J. Res. Natl. Bur. Stand., Sect. B*, **76b**, 193 (1972).
(23) Taken from the M.Sc. thesis of D. S. Saunders, University of Toronto, 1976.

Methylene Sequence Distributions and Number Average Sequence Lengths in Ethylene–Propylene Copolymers

James C. Randall

Phillips Petroleum Company, Research and Development, Bartlesville, Oklahoma 74004.
Received July 5, 1977

ABSTRACT: A direct ^{13}C NMR quantitative method is presented for measuring ethylene–propylene mole fractions and methylene number average sequence lengths in ethylene–propylene copolymers. In contrast to previous studies, the polymer is viewed as a succession of methylene and methyl-branched methine carbons as opposed to a succession of ethylene and propylene units. Problems associated with propylene inversion and comonomer sequence assignments are avoided. A methylene sequence distribution from one to six and longer consecutive methylene carbons is given for five different ethylene–propylene copolymers and can be used to distinguish copolymers which have either random, blocked, or alternating comonomer sequences.

Carbon-13 NMR has been used successfully to measure comonomer distributions and number average sequence lengths in copolymers. Unlike connecting monomer units give resonances which can be distinguished from those from like connecting units. This result leads to comonomer distributions normally described as dyads or triads of connecting monomer units and to number average sequence lengths for runs of like monomer additions. Analyses of ^{13}C NMR copolymer spectra for sequence distributions can be complicated if monomer unit inversion is present or if one of the monomer units can exist in more than a single configuration.

Ethylene–propylene copolymers are an example of a system where the propylene units may be inverted[1,2] and also exist as either meso or racemic pairs.[3,4] From a structural viewpoint, these systems may be considered terpolymers when inversion is present.[5] In analyses of sequence distributions, one customarily divides the polymer conceptually into a succession of ethylene and propylene units. Difficulties arise with propylene unit inversion because the comonomer succession cannot be uniquely described. For example, consider the following structural entities where an ethylene unit is denoted by an E and a propylene unit is denoted by either $\vec{P}$ or P depending upon whether the sequence is "tail-to-head" or "head-to-tail", respectively. Note that the presence of an even number of methylene carbons between methine carbons indicates the presence of propylene inversion; however, a unique structural entity such as the methine–methylene–methylene–methine carbon sequence cannot be described by a single succession of ethylene and propylene units.

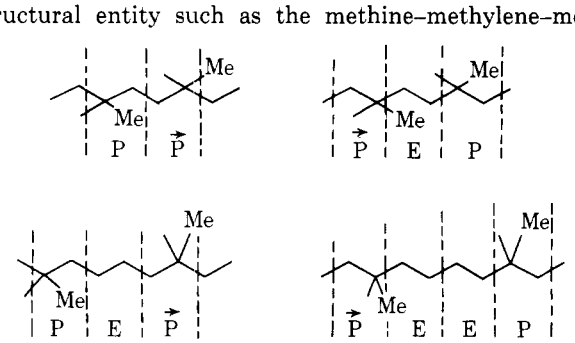

Carman, Harrington, and Wilkes[5] approached the problem of monomer unit inversion by identifying each structural sequence observed by ^{13}C NMR and considering all possible ethylene–propylene sequential assignments. Each resonance intensity was described by a linear combination of contributing species of ethylene and propylene units. Carman and co-workers then assumed first-order Markovian behavior and defined the concentration of each ethylene–propylene sequence by an appropriate set of transition probabilities. The entire ^{13}C NMR spectrum was used as a data set for obtaining values for the transition probabilities via a linear regression analysis. A complete structural determination was obtained in the form of sequence distributions, reactivity ratios, and quantitative estimates of propylene inversion.

The method used by Carman et al.[5] is not a direct measurement of the comonomer distribution but depends upon both the quality of the first-order Markov fit and the likelihood of the copolymer conforming to first-order Markov statistics. Although the latter assumption is reasonable, a more direct approach may be desirable for routine applications. However, the information offered by a direct analysis is limited primarily to sequence distributions as pointed out earlier by Carman and Wilkes.[1] The purpose of this study is to offer a method where the ethylene/propylene ratio and number average sequence lengths are determined directly and independently of propylene inversion or conformity to any particular statistical behavior.

Experimental Section

A series of five commercial ethylene–propylene copolymers are examined in this study. Copolymers A, B, and E are from Exxon, C is from Copolymer Corp. and D is from Uniroyal. The ^{13}C NMR spectra were recorded at 25 MHz and 125 °C on a Varian XL-100 NMR spectrometer equipped with a Varian 16K, FT-100 pulsed Fourier transform system and disk accessory. Instrument conditions were: pulse angle, 90°; pulse delay, 9.7 s; acquisition time, 1.5 s; and sweep width, 5000 Hz. No special precautions were made with respect

0024-9297/78/2211-0033$01.00/0